Rare Metal Materials and Engineering
Volume 50, Issue 7, July 2021
Available online at www.rmme.ac.cn

Science Press

Cite this article as: Yan Liangming, Hu Qiang, Wang Wenbo, et al. Evolution of Microstructure, Mechanical Properties and Homogeneity of Al-Zn-Mg-Cu-Zr Alloy Plates Prepared by Different Percentage Reductions per Pass[J]. Rare Metal Materials and Engineering, 2021, 50(07): 2315-2320.

ARTICLE

Evolution of Microstructure, Mechanical Properties and Homogeneity of Al-Zn-Mg-Cu-Zr Alloy Plates Prepared by Different Percentage Reductions per Pass

Yan Liangming[1,2], Hu Qiang[1], Wang Wenbo[1], Hou Xiaohu[1,2], Xu Junrui[1,2], Liu Huimin[1,2], Shen Jian[3]

[1] School of Materials Science and Engineering, Inner Mongolia University of Technology, Hohhot 010051, China; [2] Inner Mongolia Key Laboratory of Light Metal, Hohhot 010051, China; [3] GRINM Group Co., Ltd, Beijing 100088, China

Abstract: The effects of percentage reduction per pass (PRPP) on the effective strain, microstructure, mechanical properties and through-thickness homogeneity of AA7055 alloy plates were investigated through experiments and numerical simulations. Results show that with consistent total strain, the difference between the effective strain values in the surface and middle layer of AA7055 alloy plates decreases with the increase of PRPP. In the plate rolled with small PRPP, the surface layer of plate contains higher recrystallization fraction, while the middle layer comprises of large recrystallized grains. In contrast, the plate rolled with large PRPP has consistent recrystallized grain size with consistent recrystallization fraction along the thickness direction. Thus, an improved homogeneity of the microstructure and mechanical properties along the plate thickness direction can be obtained through the rolling process with large PRPP.

Key words: Al-Zn-Mg-Cu alloy; mechanical properties; homogeneity; microstructure

Al-Zn-Mg-Cu aluminum alloy thick plates with high-strength and low density were extensively used in aerospace[1-3]. Homogeneity of microstructures and mechanical properties is an important consideration during the rolling process of Al-Zn-Mg-Cu alloy plates[4-8]. In order to evenly generate severe plastic deformation along the sheet thickness direction, sheets of 7xxx series alloys are generally produced by asymmetric rolling[8,9]. The homogeneity of 7050 Al alloy sheet improves when thickness reduction per pass decreases during asymmetric rolling[8]. However, there are still some challenges in the asymmetric rolling process for producing thick plates of 7xxx series Al alloys, such as controlling the plate shape. In contrast, it is easy to control the symmetric rolling process which can improve the microstructure and mechanical properties of alloys[10,11]. In the case of traditional symmetric rolling, the effects of total reduction[12,13], temperature[14,15], and deformation mode[16,17] on the microstructures, textures, and mechanical properties of 7xxx series alloy plates were investigated. Increasing the total reduction leads to an enhancement in the proportion of recrystallized grains and a decrease in size of sub-grains, thereby improving the strength[12,18]. Reports also revealed that the rolling process of higher percentage reduction per pass (PRPP) can refine the grains of Mg sheets[19-21]. However, the mechanism of PRPP effects on the mechanical properties and microstructure of aluminum alloy plates prepared by symmetric rolling is unclear and needs to be further studied.

Therefore, 7055 aluminum alloy plates in this research were rolled with small and large PRPP separately. The effective strain distribution was analyzed by finite element (FE) analysis. The influence of PRPP on the microstructures was studied by electron back-scattering diffraction (EBSD) and transmission electron microscopy (TEM). Mechanical properties were investigated by tensile tests. Finally, the effects of

Received date: November 08, 2020
Foundation item: National Natural Science Foundation of China (51764043, 11762014); Scientific and Technological Program of Innovation and Guidance of Inner Mongolia (KCBJ2018017); Inner Mongolia Youth Talent Program of Science and Technology (NJYT-20-A16); Science Program for Returned Chinese Scholars of Inner Mongolia
Corresponding author: Yan Liangming, Ph. D., Professor, School of Materials Science and Engineering, Inner Mongolia University of Technology, Hohhot 010051, P. R. China, E-mail: yanliangming@126.com

PRPP on uniformity along thickness direction of AA7055 plates were investigated.

1 Experiment

The chemical composition of the AA7055 aluminum alloy in this study is listed in Table 1. After homogenization at 470 °C for 24 h, AA7055 ingot was machined into a cuboid specimen with a height of 60 mm. Samples were firstly heated to 430 °C and held for 20 min, and then rolled at 410 °C. The specimens were finally rolled to a height of 12 mm by small PRPP (process-I) and large PRPP (process-II) separately, as listed in Table 2. These rolled plates were solution treated at 470 °C for 70 min and 480 °C for 20 min, and immediately aged at 120 °C for 24 h. Specimens of surface layer and middle layer for the microstructure observation and the tensile tests were cut at specific position, as shown in Fig.1.

Table 1 Chemical composition of AA7055 Al alloy (wt%)

Zn	Mg	Cu	Zr	Mn	Al
7.80	2.20	2.23	0.10	0.1	Bal.

Microstructures of the plates were observed by TEM operated at 180 kV and a SSX-550 scanning electron microscope (SEM) equipped with an HKL Technology Channel5 EBSD system. TEM specimens were prepared by machining the discs of 3 mm in diameter and thinning them to 50 μm in thickness. The specimens were then treated by twin-jet electropolishing using a solution of 1vol% HF+2vol% HCl+3vol% HNO_3 at -20 °C. EBSD specimens sectioned along the normal direction (ND) -rolling direction (RD) plane were also prepared by electro-polishing with the same solution at -20 °C after mechanical polishing.

Tensile tests were conducted on a MTS810 tester at room temperature. Flaky test specimens were prepared according to the GB/T228.1-2010 standard[22], as shown in Fig.2.

FE simulations of the rolling process were performed using the FORGE FE analysis software package. The rollers were considered as rigid bodies. Because the deformation of rollers is far less than that of rolling plate, it will not be discussed in this research. The flow stress model of AA7055 alloy used in the study comes from Ref.[23]. The related rolling parameters obtained from the earlier reports[9,24-26] are listed in Table 3.

Table 2 Rolling process parameters (mm)

Process	Rolling schedule
I	60→58.44→56.88→55.28→53.68→52.12→49.88→47.49→44.31→41.16→38→34.82→31.67→28.5→26.37→22.2→19→15.6→12
II	60→58→55→52→48→43→37→31→24→17→12

2 Results and Discussion

2.1 Microstructure of rolled AA7055 alloy

Fig.3 shows the typical microstructure along the transverse direction (TD) -ND plane (TD-ND section) of the as-rolled AA7055 plate. It is found that grains are elongated along the transverse direction, resulting in the cake-like structure. Also the inhomogeneity in the sizes of the deformed grains along the thickness direction is evident, as shown in Fig.3a and 3b. Orientation imaging microscope (OIM) image of the plate surface layer rolled by process-I shows that the largest grain size along thickness direction is around 60 μm, and the grains with the size of 30~40 μm account for 60%, as shown in Fig. 3a. At the initial grain boundary, there are some recrystallized grains with the size of 2~15 μm, and the volume fraction of recrystallized grain is 20%. Fig.3b shows the OIM map of the plate middle layer rolled by process-I. The size of

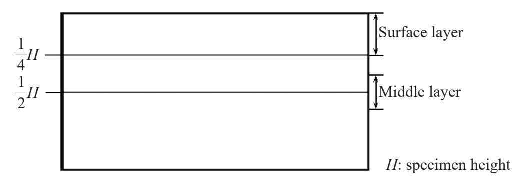

Fig.1 Schematic diagram of specimens of surface and middle layers

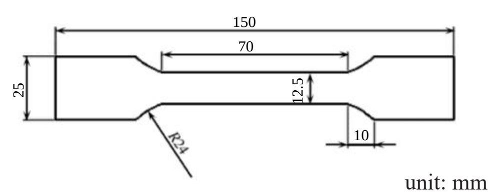

Fig.2 Standard test specimen for tensile test

Table 3 Related rolling process parameters

Parameter	Value	Ref.
Temperature/°C	410	-
Work roll radius/mm	500	-
Work roll angular velocity/rad·s^{-1}	3.2	[24]
Friction coefficient	0.35	[9], [24]
Coefficient of thermal conductivity between the rolls and plate/W·m^{-2}·K^{-1}	182.8	[26]
Young’s modulus/GPa	31.5	[24]
Poisson’s ratio	0.3	[25]

deformed grain significantly varies along the thickness direction, and some grains have a large size of ~100 μm, which is similar to the situation of as-homogenized grains. The volume fraction of recrystallization is 12%, and the recrystallized grain size is smaller. The volume fraction of recrystallized grains with the size more than 8 μm is about 6%. Fig. 3c shows the OIM map of the plate surface layer rolled by process-II. The largest size of deformed grain reaches 60 μm, and the grains with the size of 30~40 μm account for 70%. There are many recrystallized grains with sizes of ~10 μm at the original grain boundary. The volume fraction of recrystallized grains is 15% and the size is less than 5 μm. Fig. 3d shows the OIM map of middle layer of the plate rolled by process-II. The volume fraction of recrystallization reaches 12% and the maximum size of the deformed grains along the thickness direction is ~60 μm. From Fig. 3c and 3d, it is evident that the grain size along the thickness direction of the plate prepared by process-II is more homogenous than that of the plate produced by process-I.

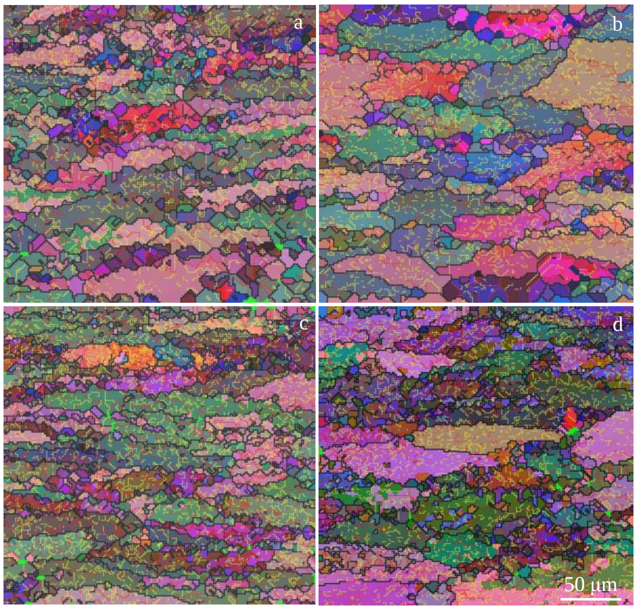

Fig.3 OIM maps of surface (a, c) and middle (b, d) layers of AA7055 alloys rolled by process-I (a, b) and process-II (c, d)

2.2 Microstructure of solution-treated plate

Fig. 4 shows the grain boundary maps and grain size distribution of rolled AA7055 plates after solution treatment. The plate rolled by process-I exhibits a recrystallization fraction of 51% in surface layer (Fig. 4a_1) and 3% in middle layer (Fig. 4b_1). The average grain size is around 34 μm in surface layer (Fig. 4a_2) and 40 μm in middle layer (Fig. 4b_2). For the plate rolled by process-II, the recrystallization fraction is about 44% in surface layer (Fig. 4c_1) and 39% in middle layer (Fig. 4d_1). The average grain size is about 32 μm (Fig.4c_2) in surface layer and 37 μm in middle layer (Fig.4d_2).

2.3 Mechanical properties

Tensile strength and elongation of the T6-treated AA7055 alloy plate are shown in Fig. 5. It is evident that the mechanical properties are influenced by the microstructure shown in Fig. 4. Compared with that of the middle layer, the tensile strength at surface layer of plate rolled by process-I increases by 5.45%, whereas as the elongation increases by 9.68%. However, the tensile strength and elongation of the surface layer of the plate rolled by process-II are 1.42% and 4.37% larger than those of the middle layer of the plate rolled by process-II, respectively. The difference of mechanical properties between the surface and middle layers for the plate rolled by process-II is less than those of the plate rolled by process-I.

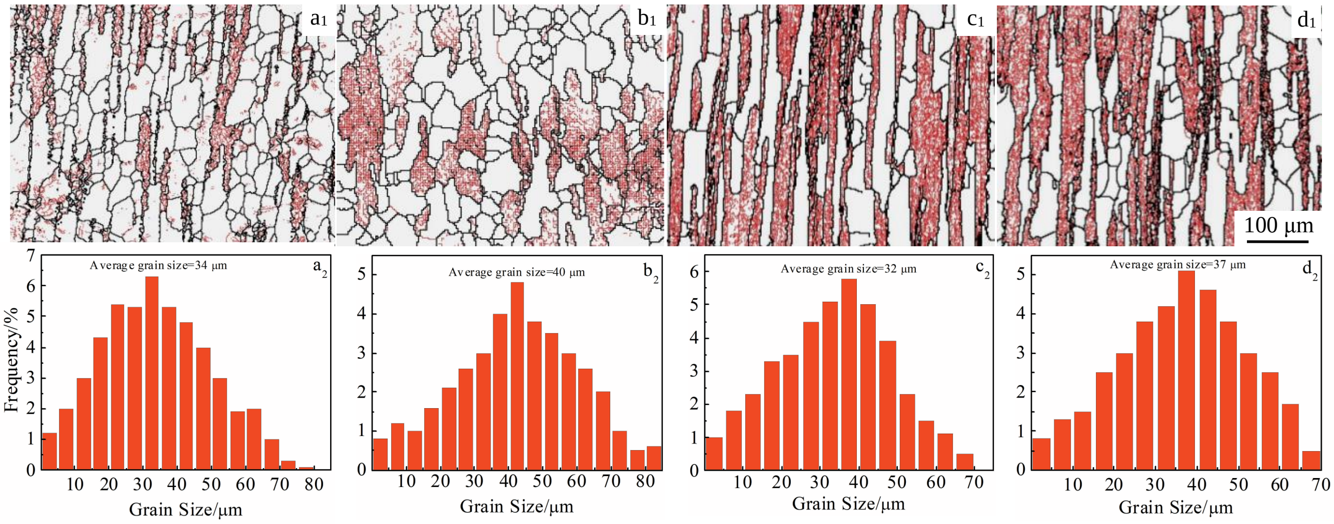

Fig.4 Grain boundary maps (a_1, b_1, c_1, d_1) and grain size distribution (a_2, b_2, c_2, d_2) of solution-treated AA7055 alloys: (a_1, a_2) surface layer of plate rolled by process-I; (b_1, b_2) middle layer of plate rolled by process-I; (c_1, c_2) surface layer of plate rolled by process-II; (d_1, d_2) middle layer of plate rolled by process-II

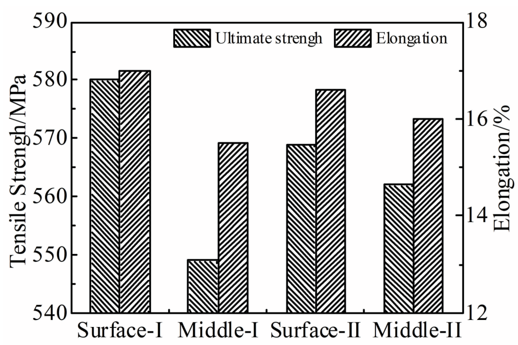

Fig.5 Mechanical properties of AA7055 alloy plates rolled by different processes

2.4 Effect of PRPP on uniformities

Results show that the uniformities of microstructure and mechanical properties along the thickness direction of AA7055 alloy plate are affected by PRPP. From Fig.3~5, it is observed that the mechanical properties and microstructures along the thickness direction in AA7055 plate prepared by both processes are obviously nonuniform. However, the large PRPP can improve the uniformity of AA7055 plate. Microstructure and mechanical properties in plate are relative to strain distribution[8,27,28]. Fig. 6 shows the equivalent strain contours of the rolled AA7055 plates. The equivalent strain of the surface and middle layers of the plate rolled by process-I is 0.768 and 0.511, respectively, as shown in Fig. 6a. The equivalent strain difference between the surface and middle layer is 0.257. The large accumulative strain is beneficial to breaking the coarse second phase, which improves the second phase dissolution during the solid solution and precipitation after aging treatment, improving the mechanical properties[5,18]. A large amount of accumulative strain causes the formation of fine grains and sub-grains (Fig.3a) and high deformed storage energy in the surface layer of AA7055 plate rolled by process-I. High deformed storage energy provides a large number of recrystallization sites during the solution treatment, resulting in a large recrystallization fraction (Fig. 4a_1). However, the lower strain accumulation and deformed coarse grains in the middle layer lead to fewer recrystallization sites and that recrystallized grains locally grow (Fig.4b_1) during the solution treatment. The plate rolled by process-II has equivalent strain of 0.717 in surface layer and 0.563 in the middle with the strain difference of 0.154. The strain distribution along thickness direction in plate rolled by process-II is more uniform than that in plate rolled by process-I. A relatively homogenous strain distribution leads to the uniform microstructure and mechanical properties.

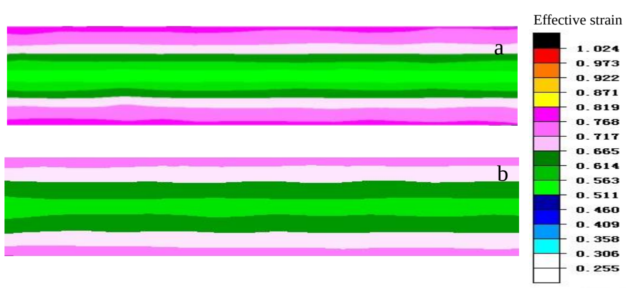

Fig.6 Effective strain distribution along longitudinal cross-section of AA7055 alloy plate rolled by process-I (a) and process-II (b)

2.5 Effect of PRPP on recrystallization after solid solution

For as-homogenized AA7055 alloy, the grains are nearly equiaxed, and the distribution of Al_3Zr dispersoid is inhomogeneous. The density of Al_3Zr dispersoid gradually decreases from the grain center to the grain boundary and becomes almost none in the area close to the boundary (Fig.7). A similar phenomenon has been reported recently for 7xxx series alloys[29-32]. After rolling, the Al_3Zr particles are concentrated in the grain center, while the coarse second phase particles are distributed along the grain boundaries parallel to the rolling direction. During the solid solution, new grains nucleate near the grain boundary by strain induced boundary migration (SIBM) and/or particle stimulated nucleation (PSN)[33,34] and grow into the initial grain. Growth of the new grains stops when the new grain boundaries are hindered by Al_3Zr particle[30].

The plate prepared by process-I has the same total reduction as the plate produced by process-II does. However, the central grain size of the plate rolled by process-I along the normal direction is larger than that of plate rolled by process-II. Thus, the distribution of Al_3Zr particles in the plate rolled by process-I is different from that of the plate rolled by process-II. Fig. 8 shows the distribution model of Al_3Zr particles in different plates. The distance along the normal direction between the precipitation free zones (PFZs) of Al_3Zr particles in the plate rolled by process-I is greater than that in plate rolled by process-II. The new grain boundaries in the plate rolled by process-II are hindered by Al_3Zr particles when the new grain size is relatively small. Hence, the grain size in plate rolled by process-II is smaller than that of the plate rolled by process-I.

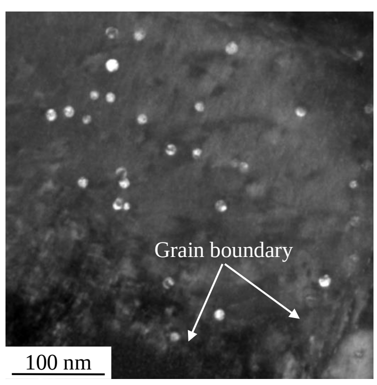

Fig.7 Al_3Zr particles in as-homogenized AA7055 alloy

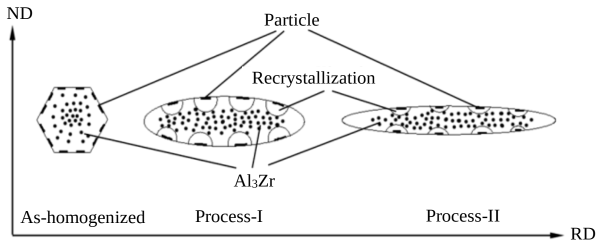

Fig.8 Schematic diagram of Al_3Zr particles distribution in grains of different plates

3 Conclusions

1) The percentage reduction per pass (PRPP) significantly affects the strain distribution of AA7055 plate, which is consistent with the microstructure and mechanical properties.

2) The homogeneity of effective strain is significantly improved by the rolling process of large PRPP, leading to different recrystallization behavior.

3) The volume fraction of recrystallized grain increases with the increase of effective strain, resulting in the increase of homogeneity of recrystallized grain in volume fraction and in grain size for the plate prepared by large PRPP.

4) The tensile strength, elongation, and homogeneity of AA7055 plate along thickness direction also improve after the process of large PRPP.

References

1 Zhang Xinming, Deng Yunlai, Zhang Yong. *Acta Metall Sin*[J], 2015, 51(3): 257 (in Chinese)

2 Zou J R, Hou L J, Shi J T *et al*. *Materials Characterization*[J], 2017, 130: 123

3 Yoganjaneyulu G, Anand Babu K, Vigneshwaran S *et al*. *Materials Letters*[J], 2019, 255: 126 606

4 She H, Shu D, Wang J *et al*. *Materials Characterization*[J], 2016, 113: 189

5 Ma C Q, Hou L G, Zhang J S. *Materials Science and Engineering A*[J], 2016, 657: 322

6 Zhou L, Chen S Y, Chen K H *et al*. *Applied Physics A*[J], 2019, 125(6): 1

7 Zhang Xinming, Han Nianmei, Liu Shengdan *et al*. *The Chinese Journal of Nonferrous Metals*[J], 2010, 20(2): 202 (in Chinese)

8 Ma C Q, Hou L G, Zhang J S *et al*. *Materials Science and Engineering A*[J], 2016, 650: 454

9 Zhang T, Wu Y X, Gong H *et al*. *The International Journal of Advanced Manufacturing Technology*[J], 2016, 87(1-4): 941

10 Chen S Y, Chen K H, Jia L *et al*. *Transactions of Nonferrous Metals Society of China*[J], 2013, 23(2): 329

11 Zang Q H, Chen H M, Lee Y S *et al*. *Journal of Alloys and Compounds*[J], 2020, 828: 154 330

12 Li Dongfeng, Zhang Xinming, Liu Shengdan *et al*. *Journal of South China University of Technology, Natural Science Edition* [J], 2015, 43(11): 75 (in Chinese)

13 Lin Lianghua, Liu Zhiyi, Han Xiangnan *et al*. *Journal of Central South University of Technology, Science and Technology*[J], 2011, 42(10): 2990 (in Chinese)

14 Yan L M, Shen J, Li Z B *et al*. *Transactions of Nonferrous Metals Society of China*[J], 2013, 23(3): 625

15 Li Junpeng, Shen Jian, Yan Xiaodong *et al*. *The Chinese Journal of Nonferrous Metals*[J], 2008, 18(11): 1951 (in Chinese)

16 Mehta K K, Mukopadhyay P, Mandal R K *et al*. *Metallurgical and Materials Transactions A*[J], 2014, 45(8): 3493

17 Lu Ruilong, Zhao Xiaodong, Lin Jinbao *et al*. *Rare Metal Materials and Engineering*[J], 2015, 44(12): 3094 (in Chinese)

18 Huang D M, Shen Y M, Yuan Q *et al*. *Materials Research Express*[J], 2019, 6(11): 115 021

19 Guo J Q, Yang H, Liu P *et al*. *Rare Metals*[J], 2017, 36(11): 912

20 Xu H B, Tang S, Xi H F *et al*. *Rare Metals*[J], 2017, 36(11): 872

21 Yim C D, Seo Y M, You B S. *Metals and Material International* [J], 2009, 15(4): 683

22 Standardization Administration of the P. R. C. GB/T 228.1-2010 [S], 2010

23 Yan L M, Shen J, Li J P *et al*. *International Journal of Minerals Metallurgy and Materials*[J], 2010, 17(1): 46

24 Fu Y, Xie S S, Xiong B Q *et al*. *Journal of Wuhan University of Technology, Mater Sci Ed*[J], 2012, 27(2): 247

25 Xu L, Dai G Z, Huang X M *et al*. *Applied Mechanics and Materials*[J], 2012, 1799: 896

26 Fu Yao. *Thesis for Doctorate*[D]. Beijing: General Research Institute for Nonferrous Metals, 2011 (in Chinese)

27 Deng Y L, Zhang Y Y, Wan L *et al*. *Materials Science & Engineering A*[J], 2012, 54(5): 33

28 Becerra G, Ramos-Grez J, Montecinos J. *Journal of Materials Engineering and Performance*[J], 2009, 18(8): 1144

29 Lu X Y, Guo E G, Rometsch P *et al*. *Transactions of Nonferrous Metals Society of China*[J], 2012, 22(11): 2645

30 Zhang Y, Bettles C, Rometsch P A. *Journal of Materials Science* [J], 2014, 49(4): 1709

31 Yu X X, Sun J, Li Z T *et al*. *Materials Research Express*[J], 2018, 6(2): 26 574

32 Xie Z Q, Jia Z H, Xiang K Y *et al*. *Metallurgical and Materials Transactions A, Physical Metallurgy and Materials Science*[J], 2020, 51(10): 5378

33 Nobakht S, Kazeminezhad M. *International Journal of Minerals Metallurgy and Materials*[J], 2017, 24(10): 1158

34 Zhao J H, Deng Y L, Tan J *et al*. *Materials Science & Engineering A*[J], 2018, 734: 120

道次压下率对 Al-Zn-Mg-Cu-Zr 合金组织、力学性能及均匀性的影响

闫亮明[1,2]，胡　强[1]，王文波[1]，侯小虎[1,2]，徐俊瑞[1,2]，刘慧敏[1,2]，沈　健[3]

(1. 内蒙古工业大学 材料科学与工程学院，内蒙古 呼和浩特 010051)

(2. 内蒙古轻金属材料重点实验室，内蒙古 呼和浩特 010051)

(3. 有研科技集团有限公司，北京 100088)

摘　要：通过实验和数值模拟的方法研究了道次压下率（PRPP）对 7055 铝合金板材的应变分布、微观组织、力学性能及其沿厚度方向的均匀性的影响。结果表明，总变形量相同的情况下，增大道次压下率，可以减小 7055 铝合金板材表层与中间层之间的等效应变差。道次压下率较小的工艺轧制板材的表层比中间层的再结晶比例高，并且中间层有尺寸较大的再结晶晶粒。然而，经道次压下率较大的工艺轧制的板材沿厚度方向有均匀的再结晶比例和再结晶晶粒尺寸。因此，道次压下率较大的轧制工艺可以提高板材组织和力学性能的均匀性。

关键词：Al-Zn-Mg-Cu 合金；力学性能；均匀性；微观组织

作者简介：闫亮明，男，1979 年生，博士，教授，内蒙古工业大学材料科学与工程学院，内蒙古 呼和浩特 010051，E-mail：yanliangming@126.com